J Mater Sci: Mater Electron (2017) 28:3515–3522
DOI 10.1007/s10854-016-5951-x

Electrochemical synthesis of polyaniline/inorganic salt binary nanofiber thin films for electrochromic applications

Y. E. Firat[1,2] · A. Peksoz[1]

Received: 25 August 2016 / Accepted: 24 October 2016 / Published online: 31 October 2016

Abstract Polyaniline conductive polymer thin films without or with $LiClO_4$ inorganic salt were coated by electrochemical deposition method on ITO surface. Electrochromic stability test, electrochemical behavior, coloring performance, optical properties and surface formations of the produced films were studied in detail. The deposited films were found to have a good stability. Electrochemical analysis showed that the conductivity of $LiClO_4$ doped PANI film was higher than that of the PANI. Oxidation and reduction peaks, and potentials differed significantly depending on the content of the electrolytes. SEM studies demonstrated that the surface of each film consisted of completely nanofibers. Addition of $LiClO_4$ to the deposition electrolyte decreased substantially the diameter of these nanofibers. PANI film with $LiClO_4$ exhibited four colors, while pure PANI film had three different colors. The EDX results obtained from the surface of $LiClO_4$ doped PANI material indicated that PANI and $LiClO_4$ could be successfully linked to form PANI/LiClO4 binary thin film.

1 Introduction

Electrochromic windows (ECWs), also known as "smart windows" or "smart glass", are related to the reversible change in optical properties of a material induced by oxidation (loss of electrons) and reduction (gain of electrons) due to externally applied potential difference in an amplitude of approximately 3 V DC.

Typical ECW consists of five layers of GS/TC/EC/IC/IS/TC/GS, where GS is a glass substrate, TC is a transparent conductor, EC is an electrochromic coating, IC is an ion conductor and IS is an ion storage coating [1]. According to the applications, the GS/TC can be preferred as a transparent or reflective coating. In the transitive EC windows, many transparent electronic conductors (TC) can be used such as ITO (indium tin oxide), FTO (fluorine tin oxide) or ATO (antimony tin oxide). Among these conductors, ITO is suitable material in terms of optical and electrical properties. Electrochromic material layer is the most important part of ECW due to the changing of its color after being applied a potential. For the last decade, several inorganic electrochromic materials and organic electrochromic materials have been extensively studied [2, 3]. Organic electrochromic material is more attractive compared with inorganic electrochromic materials due to the advantages in low costs, the short response time and the multiple color changes [4, 5]. Conducting polymer films have been widely used as organic electrochromic material. Among the conducting polymers, polyaniline (PANI) exhibits additional physical and chemical properties such as excellent environmental stability, easy deposition, stability in aqueous solutions and relatively high level of electrical conductivity [6]. PANI has been used in several applications, such as biochemical sensors, rechargeable batteries, sensors, electrochromic windows, electromagnetic interference shielding and corrosion protection [5–7]. PANI has four redox states with different colors which are, yellow colored leucoemeraldine base (LB, fully reduced state), green colored emeraldine salt (ES, half oxidized state), blue colored emeraldine base (EB, half oxidized

✉ A. Peksoz
peksoz@uludag.edu.tr

[1] Solar Cell Laboratory, Physics Department, Faculty of Arts and Sciences, Uludag University, Gorukle Campus, 16059 Bursa, Turkey

[2] Physics Department, Kamil Ozdag Faculty of Sciences, Karamanoglu Mehmetbey University, Yunus Emre Campus, 70100 Karaman, Turkey

state) and finally, violet colored pemigraniline base (PB, fully oxidized state) [8].

PANI can be prepared by chemical or electrochemical process through oxidative polymerization of aniline monomer. The electrochemical polymerization is one of the most common methods in producing adherent and uniform thin polymer films. Thickness, conductivity and coloring quality of the films can be controlled by changing the synthesis parameters, including the current density, substrate, pH, nature and concentration of electrolyte [9]. These are the advantageous sides of electrochemical polymerization method.

Here, we report electrochemical deposition of PANI on ITO coated glass substrate in hydrochloric acid solutions with or without $LiClO_4$ inorganic salt. Considerably innovative information on the new produced PANI film characteristics depending upon inorganic salt is given to the literature by evaluating the results coming from our experiments and by comparing early works. To our knowledge, this is the first report to synthesize PANI/lithium perchlorate salt binary thin films. This binary nanofiber thin film is expected to have a high conductivity and a good electrochemical activity.

2 Experimental

2.1 Material

Aniline ($C_6H_5NH_2$, 99.5% purity), hydrochloric acid (HCl), sulfuric acid (H_2SO_4) and lithium perchlorate ($LiClO_4$) were purchased from Sigma-Aldrich. All chemicals were used as received and pure water was used for all aqueous solutions. A transparent ITO coated glass was used as a substrate with a surface area of 1 cm × 1 cm and a sheet resistance of 0–10 Ω/cm^2. Prior to the deposition, the substrates were cleaned with acetone and then pure water using ultrasonic cleaner in order to remove any adsorbed substances on the electrode surface for a better adhesion of the films. Finally, the cleaned substrates were dried to be ready for the film deposition.

2.2 Syntheses of polyaniline/inorganic salt binary thin films

All electrochemical experiments were performed with a Gamry Reference 3000 Potentiostat/Galvanostat. A schematic illustration of the electrodeposition system was given in Fig. 1. This deposition system has a conventional three-electrode configuration: ITO-coated glass as a working electrode, platinum wire as a counter electrode and Ag/AgCl as a reference electrode. Cyclic voltammetry (CV)

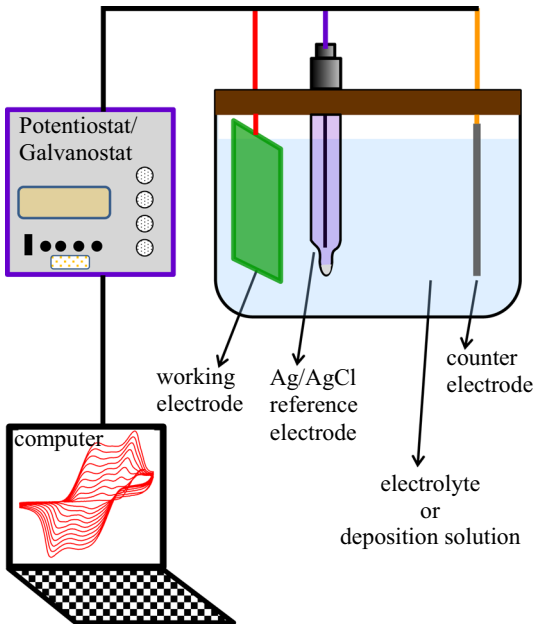

Fig. 1 Schematic illustration of electrodeposition system used in this work

was used to characterize the electrochemical behavior in aqueous solutions consisting of 0.25 M aniline and 0.5 M aqueous HCl (electrolyte I), and 0.25 M aniline, 0.1 M $LiClO_4$ and 0.5 M HCl (electrolyte II). This characterization provided the determination of the polymerization potentials of aniline on the ITO surface. The cyclic voltammetry was performed for the both electrolytes between potential limits of −0.4 and +1.2 V at 100 mV /s scan rate for ten cycles. The PANI film was electrochemically deposited on ITO substrate in both electrolytes using chronoamperometry technique at a constant potential of +0.9 V versus Ag/AgCl for 1200 s.

2.3 Measurements

Coloring performance and stability test of the produced films were performed with Gamry Reference 3000 Potentiostat/Galvanostat/ZRA. PHE200 Physical Electrochemistry software was used to operate these tests by CV technique at the room temperature. Hall-effect measurement system with four-point probe was used to determine some electrical parameters of the films (HMS-3000 Manual Ver 3.5). Scanning electron microscope (SEM) micrographs were obtained by a Carl Zeiss EVO 40 system (Carl Zeiss NTS Limited Company, Cambridge, UK). The elemental analysis was performed in Bruker AXS Microanalysis energy dispersive X-ray (EDX) analysis operated at 10 keV with XFlash 4010 detector. Ultraviolet–visible spectra (UV–Vis) were recorded with the Shimadzu UV-2600 spectrophotometer.

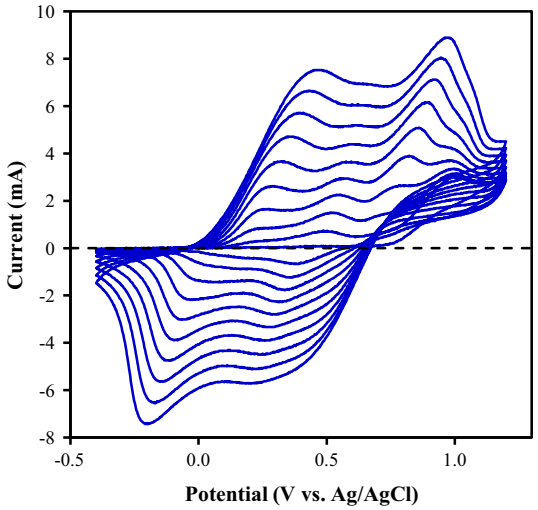

Fig. 2 Cyclic voltammetry curves of pure PANI deposition on ITO substrate in a solution of 0.25 M aniline and 0.5 M aqueous HCl for ten cycles at 100 mV/s

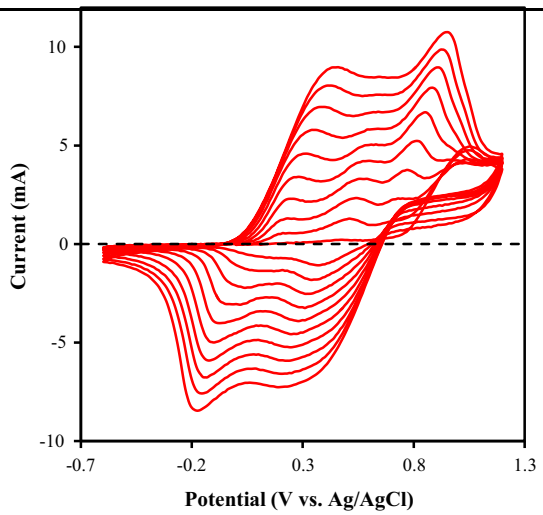

Fig. 3 Cyclic voltammetry curves of PANI–$LiClO_4$ deposition on ITO substrate in a solution of 0.25 M aniline and 0.5 M aqueous HCl and 0.1 M $LiClO_4$ for ten cycles at 100 mV/s

3 Results and discussion

3.1 Voltammetric studies

It was reported before that the CV, which is one of the electropolymerization processes, had impact on morphology of the polymer, and provided the possibility of determining the thickness and composition of the film on the substrate surface [10, 11]. The determination of the growth potentials of PANI on the ITO surface was provided by CV between −0.4 and 1.2 V at a scan rate of 100 mV/s for ten cycles in electrolyte I (Fig. 2). The increase in the redox and oxidation current intensity is an evidence of a successive growth of the PANI film, as the number of polymerization cycles changes from one to ten. There are three anodic peaks at +0.3, +0.6 and +0.9 V and two cathodic peaks at −0.178 and +0.244 V indicating the presence of discrete electroactive regions in the film. The anodic peak potentials at +0.3 and +0.9 V correspond to the formation of leucoemeraldine form to the emeraldine form and emeraldine form to the pernigrenaline form, respectively. The middle peak at the +0.6 V is unknown to our knowledge, but it may be attributed to the degradation or side product of the PANI.

Addition of 0.1 M $LiClO_4$ into the deposition bath changed the line shape of the CV. Figure 3 shows typical CV recorded between −0.6 and +1.2 V at a scan rate of 100 mV/s for ten cycles in electrolyte II. The observed maximum current was 8.76 mA (positive direction) and −7.39 mA (negative direction) in electrolyte I, while it was 10.7 mA and −8.34 in electrolyte II (Figs. 2, 3). So the current for electrolyte II is seen to be higher than that for the electrolyte I. This means that electrolyte II has more

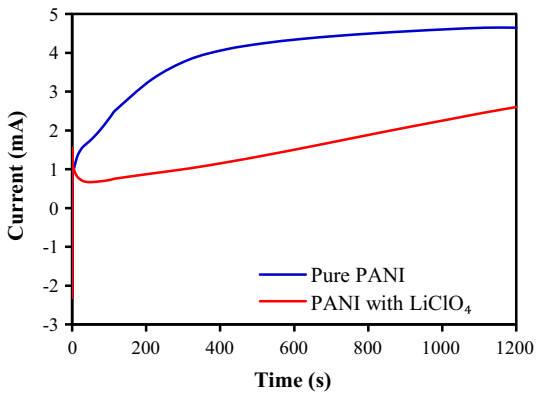

Fig. 4 Potentiostatic current–time curves recorded on ITO electrode for PANI thin films deposited in the two different electrolytes

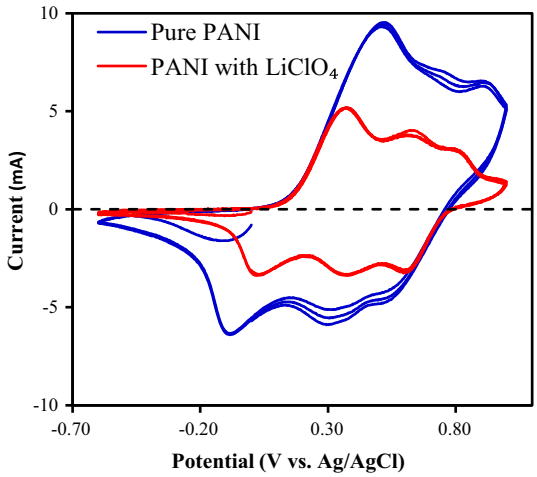

Fig. 5 Electrochromic behavior of PANI without or with $LiClO_4$ in 0.1 M H_2SO_4

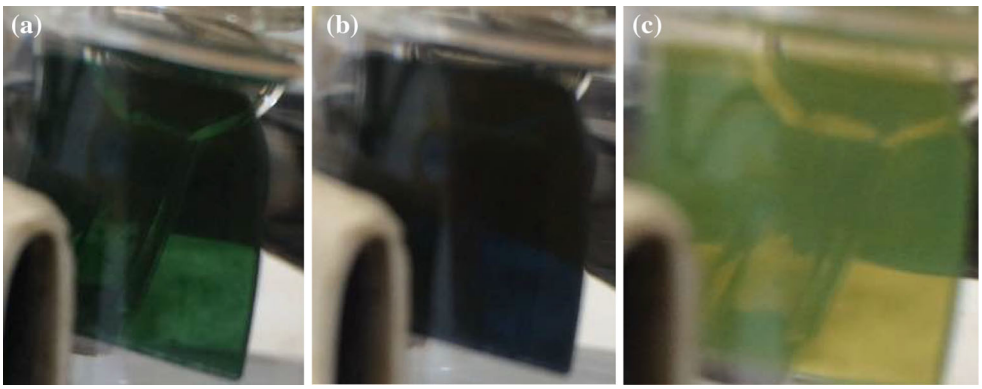

Fig. 6 Coloring of PANI film without $LiClO_4$ at a potential of **a** +0.54 V, **b** +0.88 V and **c** −0.6 V

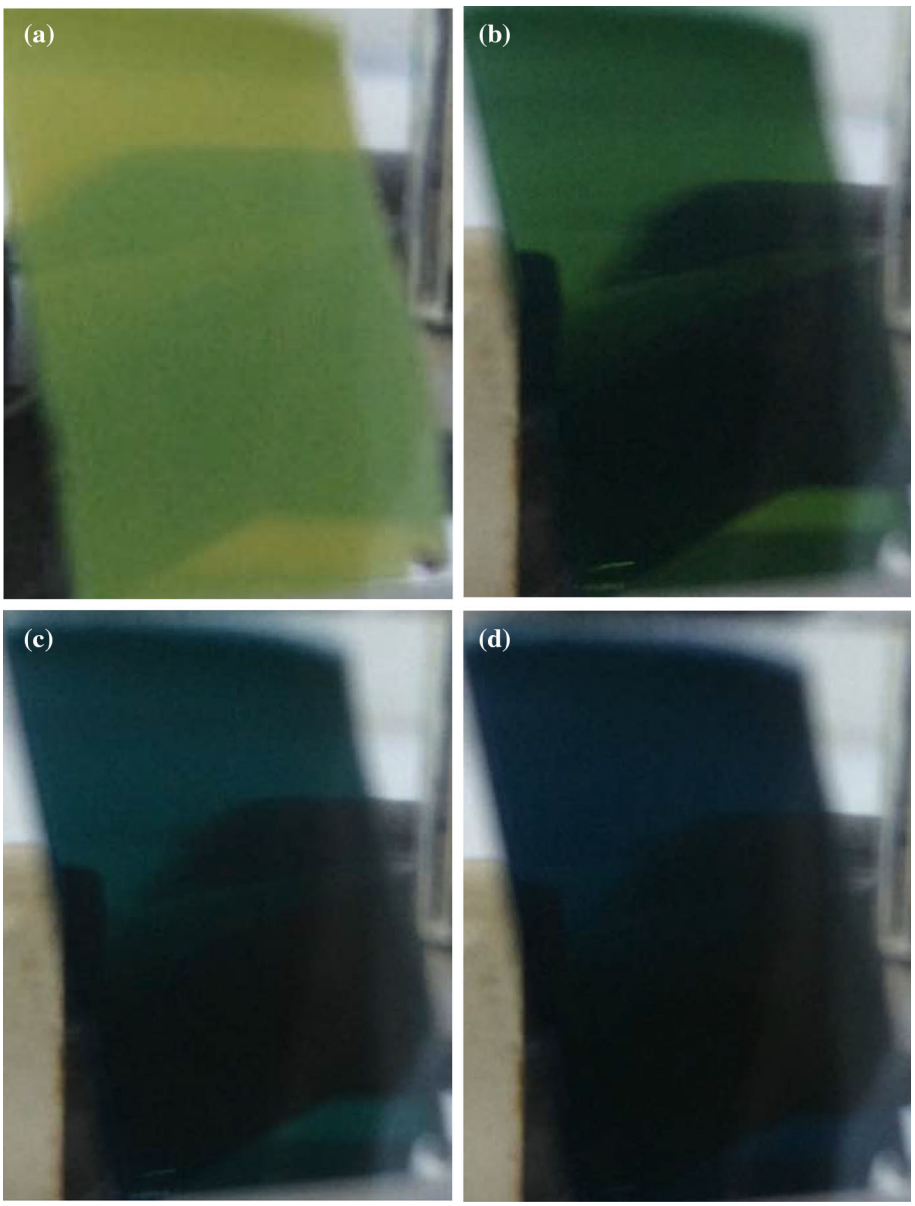

Fig. 7 Coloring of PANI film with $LiClO_4$ at a potential of **a** −0.6 V, **b** +0.40 V, **c** +0.60 V and **d** +0.85 V

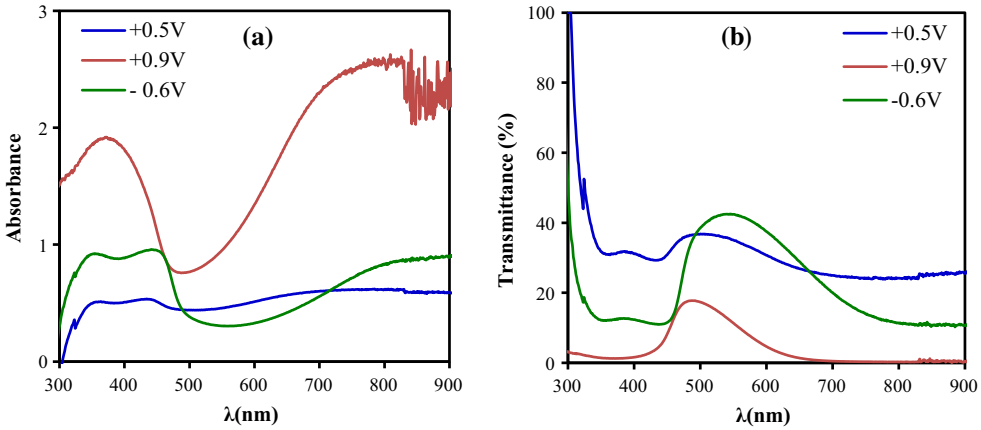

Fig. 8 **a** Absorbance and **b** transmittance spectra of PANI thin films produced in the solution without $LiClO_4$

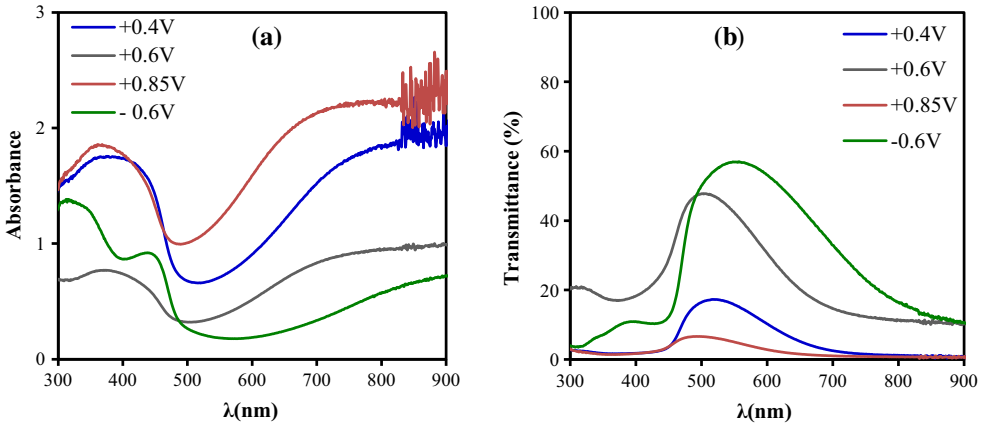

Fig. 9 **a** Absorbance and **b** transmittance spectra of PANI thin films produced in the solution with $LiClO_4$

Table 1 Coloring potential values, wavelengths corresponding to absorbance peaks, transition types of the produced PANI nanofiber thin films

Nanofiber film	Deposition solution	Coloring potential (V)	π–π* (nm)	Polaron–π* (nm)	π–polaron (nm)
PANI without $LiClO_4$	250 mM aniline	+0.54	363	434	820
	0.5 M aqueous HCl	+0.88	299	389	748
		−0.60	355	441	818
PANI with $LiClO_4$	250 mM aniline	+0.4	323	376	814
	0.5 M aqueous HCl	+0.60	292	374	778
	0.1 M $LiClO_4$	+0.85	307	361	805
		−0.60	315	438	837

electrical conductivity. Thus, more aniline was polymerized on the ITO substrate with electrolyte II. It is not observed any changes on the number of peaks in the presence of $LiClO_4$, despite of the fact that $LiClO_4$ causes the general shape of the voltammogram to be differed.

3.2 Film deposition

Figure 4 shows time–current curves for the PANI by setting the working electrode potential to +0.9 V for 1200 s in both electrolytes I and II. For the electrolyte I, the curves corresponding to the electropolymerization of the PANI can be interpreted by separating in two stages. In the first stage, the deposition current increases with time, which means the nucleation of PANI. During the second stage, the current density increases less sharply than the first stage. This corresponds to the growth of PANI on the first layer. The time–current variation exhibited a decreasing in a short time, after then it increased linearly for the PANI deposited in electrolyte II (Fig. 4).

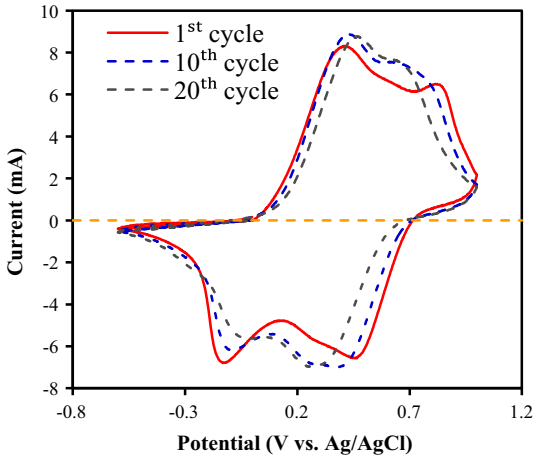

Fig. 10 Coloring stability curves of PANI without $LiClO_4$ at a scan rate of 50 mV/s

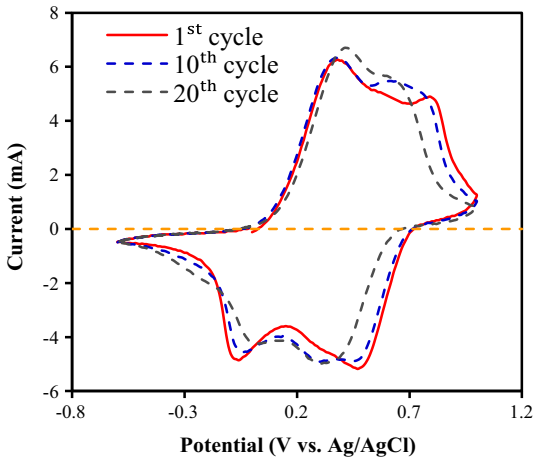

Fig. 11 Coloring stability curves of PANI with $LiClO_4$ at a scan rate of 50 mV/s

3.3 Electrochromic properties

CV was used to examine electrochemical behavior of PANI film in acidic medium. During adding and removing of H^+ ions into or from the film, PANI film gains a new redox state namely a new color. Figure 5 shows the CV characteristics of both PANI films in an aqueous solution of 0.1 M H_2SO_4 scanned between −0.6 and 1.0 V at a scan rate of 50 mV/s. As can be seen from Fig. 5, there are two oxidation peaks correspond to the transformation of emeraldine salt (ES) from leucoemeraldine base (LB) at +0.5 V and conversion of emeraldine salt (ES) to pernigraniline salt (PS) at +0.9 V. On the negative direction, PS reduced back to ES at +0.4 V and ES reduced back to LB at −0.1 V (Fig. 5).

For the CV diagram of PANI film obtained in electrolyte II (Fig. 5), there are three oxidation peaks in the positive scan at +0.4, +0.6 and +0.85 V and three reduction peaks

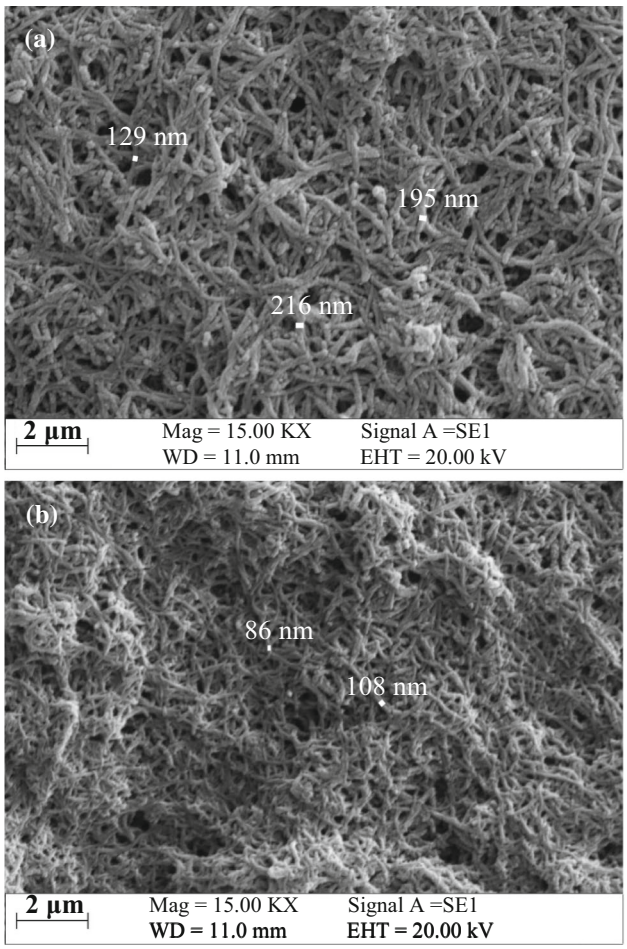

Fig. 12 SEM image of PANI film deposited from the electrolyte **a** without $LiClO_4$ and **b** with $LiClO_4$. The images were obtained in a magnification of 15,000

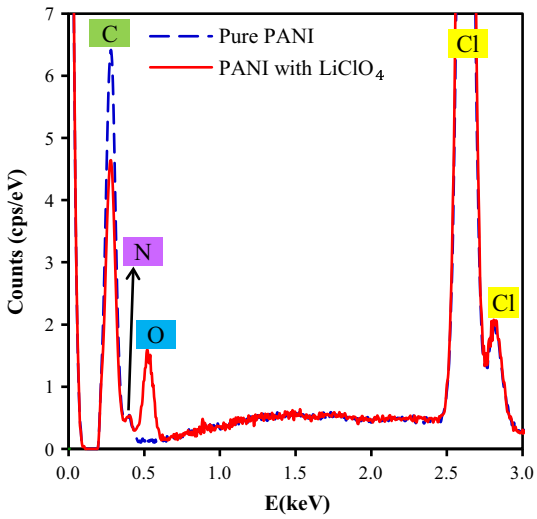

Fig. 13 EDX spectra of pure PANI and $LiClO_4$ doped PANI thin films

Table 2 EDX results of the produced PANI nanofiber thin films

Nanofiber film	Solution	C (%)	N (%)	Cl (%)	O (%)
PANI without $LiClO_4$	250 mM aniline 0.5 M aqueous HCl	51.12	41.47	7.41	0.00
PANI with $LiClO_4$	250 mM aniline 0.5 M aqueous HCl 0.1 M $LiClO_4$	32.43	23.22	8.31	36.06

in the negative scan at −0.04, +0.35 and +0.6 V, respectively. The oxidation peak at +0.4 V and the reduction peak at −0.04 V represents the change between LB and ES with doping/dedoping of the anion processes. The oxidation peak at +0.85 V and the reduction peak at +0.6 V belongs to the change between EB and PS with protonation/deprotonation processes. The middle oxidation peak at +0.6 V and reduction peak at +0.35 V might be reversible transformation process of ES to EB [12, 13].

3.4 Optical and stability tests

Coloring of PANI thin films produced in the medium without or with LiClO4 were imaged in Figs. 6 and 7. The absorbance and transmittance spectra of the PANI films recorded during these coloring states were given in Figs. 8 and 9. The absorption peaks of the deposited PANI thin films represented some shifts depending on the applied potentials due to the delocalization of the charge carrier. Figures 8 and 9 illustrate three maxima, the first localized between 300 and 363 nm, the second between 361 and 438 nm, and the third between 748 and 837 nm. The absorbance peaks, applied potential values in coloring, transition types of the PANI nanofiber films were summarized in Table 1. The first peaks of the PANI films at the all applied potentials can be attributed to π–π* transitions [14, 15]. The second peaks are due to the polaron–π* transitions. The third wide peaks observed at higher wavelengths are assignable to the π–polaron transitions [15, 16]. The stability performance of the produced films was also reported here (Figs. 10, 11). First, tenth and twentieth cycle were illustrated for each polymer film, and the results showed that the produced PANI films exhibited a good stability in 1.0 M H_2SO_4 after 20 cycles (Figs. 10, 11).

3.5 SEM and EDX analysis

The SEM images of the both PANI thin film were given in Fig. 12. Figure 12a shows the surface formations of the PANI thin film deposited from electrolyte I. The film surface from electrolyte I has nanofibrous structures and many pores, and the diameter of the nanofibers is within the range of 125–220 nm. Diameter of the nanofibers on the PANI film from electrolyte II is approximately 100 nm, and the film surface is more regular and less pores (Fig. 12b). These observations demonstrated that nanofiber diameter was decreased with the presence of $LiClO_4$ in the deposition electrolyte (Fig. 12). The nanofibers can be attributed to the interaction of para-position of aniline with ITO surface [17].

Figure 13 shows EDX spectra of pure PANI and $LiClO_4$ doped PANI thin films. The signals of the carbon (C) and nitrogen (N) elements were observed at 0.28 and 0.39 keV for both pure PANI and $LiClO_4$ doped PANI thin film, respectively. C and N peaks in EDX spectra confirm the occurrence of polymerization of aniline (Fig. 13). Oxygen (O) signal was not observed for pure PANI. As seen from Fig. 13, the O signal observed at 0.51 keV demonstrates that PANI film was doped by perchlorate ions (ClO_4^-). The chlorine (Cl) peaks at 2.62 and 2.82 keV is due to the presence of HCl in electrolyte I and the presence of HCl and $LiClO_4$ in electrolyte II. The elemental compositions of the produced films were listed in Table 2. Pure PANI film is composed of 51.12% C, 41.47% N, 7.41% Cl and 0.00% O, while $LiClO_4$ doped PANI film has 32.43% C, 23.22% N, 8.31% Cl and 36.06% O elemental compositions (Table 2).

4 Conclusions

The PANI films were successfully electropolymerized on ITO substrates from two different electrolytes without or with $LiClO_4$ inorganic salt. SEM studies showed each PANI film had nanofibers on their surfaces. The diameter of the nanofibers is approximately 100 nm for the PANI films deposited from electrolyte II, while it is 200 nm for the film from electrolyte I. The PANI film without or with $LiClO_4$ was observed to have two or three oxidation peaks, respectively. UV–Vis absorbance and transmittance spectra of the PANI films were studied depending on the coloring potentials. Electrochemical CV analysis of the deposited PANI films demonstrated that the films had an excellent coloring reversibility and high stability in acidic solution.

Acknowledgements This work was supported by the Research Fund of the Uludag University, Project Number OUAP(F)-2013/11. The authors thank to Uludag University for financial support.

References

1. Y. Ji, C. Qin, H. Niu, L. Sun, Z. Jin, X. Bai, Dyes Pigments **117**, 72 (2015)
2. N. Velhal, N. Patil, S. Jamdade, V. Puri, Appl. Surf. Sci. **307**, 129 (2014)
3. V. Meriga, S. Valligatla, S. Sundaresan, C. Cahill, V.R. Dhanak, A.K. Chakraborty, J. Appl. Polym. Sci. **42766**, 1 (2015)
4. G. Sun, X. Zhang, J. Rappich, K. Hinrichs, Appl. Surf. Sci. **344**, 181 (2015)
5. R.B. Patil, A.A. Jatratkar, R.S. Devan, Y.R. Ma, R.K. Puri, V. Puri, J.B. Yadav, Appl. Surf. Sci. **327**, 201 (2015)
6. Y. Li, Z. Li, F. Zheng, J. Appl. Polym. Sci. **42785**, 1 (2015)
7. E.A. Özerol, B.F. Şenkal, M. Okutan, Microelectron. Eng. **146**, 76 (2015)
8. L. Zhao, L. Zhao, Y. Xu, T. Qiu, L. Zhi, G. Shi, Electrochim. Acta **55**, 491 (2009)
9. M. Hatamzadeh, R.M. Rezaei, M. Jaymand, Mater. Sci. Semicond. Process. **31**, 463 (2015)
10. L. Niu, Q. Li, F. Wei, S. Wu, P. Liu, X. Cao, J. Electroanal. Chem. **578**, 331 (2005)
11. A. Mourato, A.S. Viana, J.P. Correia, H. Siegenthaler, L.M. Abrantes, Electrochim. Acta **49**, 2249 (2004)
12. W.K. Chen, C.W. Hu, C.Y. Hsu, K.C. Ho, Electrochim. Acta **54**, 4408 (2009)
13. T.H. Lin, K.C. Ho, Sol. Energy Mater. Sol. Cells **90**, 506 (2006)
14. Q. Wang, X. Qian, S. Wang, W. Zhou, H. Guo, X. Wu, J. Li, X. Wang, Synth. Met. **199**, 1 (2015)
15. M. Das, D. Sarkar, J. Mater. Sci. Mater. Electron. **27**, 4109 (2016)
16. S. Pruneanu, E. Veress, I. Marian, L. Oniciu, J. Mater. Sci. **34**, 2733 (1999)
17. H. Zhang, J. Wang, Z. Wang, F. Zhang, S. Wang, Synth. Met. **159**, 277 (2009)